Check for updates

Soil microbial CO2 fixation rate disparities with different vegetation at a representative acidic red soil experimental station in China

Chao Long[1,2], Zuwen Liu[1,2,3], Renlu Liu[1], Li Yin[1], Fuxing Tan[1], Yian Wang[1]* and Genhe He[1]*

[1]School of Life Sciences, Key Laboratory of Jiangxi Province for Functional Biology and Pollution Control in Red Soil Regions, Jinggangshan University, Ji'an, Jiangxi, China, [2]School of Civil and Surveying & Mapping Engineering, Jiangxi University of Science and Technology, Ganzhou, Jiangxi, China, [3]School of Hydraulic & Ecological Engineering, Nanchang Institute of Technology, Nanchang, Jiangxi, China

Soil acidification poses a significant environmental challenge in China's southern red soil regions, impacting the abundance of soil microbes and their capacity for carbon fixation. The effect of vegetation types on soil's biological and abiotic components under acidification, and their regulatory role on the CO_2 fixation mechanisms of soil autotrophic microorganisms, is difficult to examine. This gap in understanding constrains the assessment of the carbon fixation potential of red soils. To address this, indoor cultivation coupled with ^{13}C stable isotope labeling was employed to evaluate the disparate abilities of autotrophic microorganisms to assimilate and store CO_2 across five vegetation soils from the Qianyanzhou acidic red soil experimental station in China. Findings indicate that carbon fixation rates in these soils spanned from 4.25 to 18.15 mg C kg^{-1} soil d^{-1}, with paddy field soils demonstrating superior carbon fixation capabilities compared to orchard, coniferous forest, broad-leaved forest, and wasteland soils. The ^{13}C fixation rate in the 0−10 cm soil stratum surpassed that of the 10−30 cm layer across all vegetation types. High-throughput sequencing of 16S rRNA, following *cbbL* gene purification and amplification, identified *Bradyrhizobium*, *Azospirillum*, *Burkholderia*, *Paraburkholderia*, and *Thermomonospora* as the predominant autotrophic carbon-fixing microbial genera in the soil. PERMANOVA analysis attributed 65.72% of the variance in microbial community composition to vegetation type, while soil depth accounted for a mere 8.58%. Network analysis of microbial co-occurrence suggested the soil microbial interactions and network complexity changed with the change of vegetation types. Additionally, multiple linear regression analysis pinpointed the Shannon index and soil organic carbon (SOC) content as primary influencers of carbon fixation rates. Structural equation modeling suggested that iron enrichment and acidification indirectly modulated carbon fixation rates by altering SOC and autotrophic bacterial diversity. This investigation shows the spatial dynamics and mechanisms underpinning microbial carbon fixation across varying vegetation types in southern China's red soil regions.

1 Introduction

Soil represents the most substantial carbon store within terrestrial ecosystems, offering vital ecosystem services, including agricultural productivity, water purification, and climate modulation (Anikwe and Ife, 2023). Soil microorganisms are pivotal in upholding soil functionality, thereby sustaining ecosystem services and functional stability, encompassing primary production and nutrient turnover (Banerjee et al., 2018; Bu et al., 2023). Post-industrial human endeavors have precipitated widespread soil degradation, with the world's agricultural soils forfeiting approximately 133bn tonnes of carbon, potentially impacting ecosystem productivity and atmospheric CO_2 levels (Sanderman et al., 2017). The principal contributors to soil carbon include plant detritus, root secretions, microbial biomass and necromass, alongside carbon fixation by autotrophic microbes (Mason et al., 2023). These autotrophs, as nature's quintessential biosynthetic entities, are responsible for an estimated 0.6–4.9 Pg C yr^{-1} of CO_2 fixation, equating to 25% of total anthropogenic CO_2 discharges (Bossio et al., 2020; Zheng Z. C. et al., 2022). Exhibiting remarkable adaptability across various ecosystems, they predominantly engage in the carbon cycle via the Calvin–Benson–Bassham (CBB) pathway, facilitated by the rate-limiting enzyme Rubisco (Li et al., 2020). The *cbbL* gene encodes Rubisco I's large subunit, serving as a marker for carbon-fixing microbes and is extensively utilized to evaluate soil autotrophs' CO_2 fixation capacity (Qin et al., 2021; Bu et al., 2023). However, extant research has chiefly concentrated on the influence of land stewardship and disparate soil regions on autotrophic microbial communities and their CO_2 fixation aptitude (Mukasa Mugerwa and McGee, 2017; Li et al., 2018; Zhou et al., 2019; Bu et al., 2023; Cheng et al., 2023), with a notable dearth of studies examining soil properties' effects on autotrophic microorganisms and carbon dynamics.

Occupying 36% of China's arable land, the red soil region is a critical contributor to the nation's rice production, accounting for over 90% of the output (Huang and Zhao, 2014). Predominantly found in tropical and subtropical zones, these soils are subject to frequent alternations of high temperatures and rainfall, leading to severe erosion and leaching of alkali metal ions. Consequently, this results in elevated concentrations of iron and aluminum oxides, culminating in soil acidification (Xing et al., 2022). The dissolution of stable metal mineral-soil organic matter (SOM) complexes by acid rain further influence of SOM microbial mineralization (Moore et al., 2023). While prior research has concerned the interplay between autotrophic microorganisms, soil attributes, and various factors—including regional, soil type, and agricultural management influences—on these microorganisms' carbon-fixation capabilities (Chu et al., 2016; Zhou et al., 2019; Wang et al., 2021), the feedback mechanisms and functional behaviors of autotrophic carbon-sequestering microbes in iron- and aluminum-rich acidic red soils remain largely uncharted.

Iron oxides can interact with soil organic carbon (SOC) in multiple ways: they may adsorb, complex with, and co-precipitate SOC, thereby enhancing its stabilization. Conversely, iron-reducing bacteria may facilitate dissimilatory Fe reduction, utilizing SOC and Fe as electron donors and acceptors, respectively, which can accelerate SOC decomposition (Moore et al., 2023; Yao Y. et al., 2023). Moreover, the diversity of vegetation types modulates soil physicochemical properties through processes such as litter decomposition and root exudation, subsequently affecting the composition and diversity of soil protozoa and microbial communities, as well as soil carbon-fixation rates (Bahadori et al., 2021; Bhattacharyya et al., 2022; Spohn et al., 2023; Yao Y. W. et al., 2023; Sun et al., 2024). For instance, Lynn et al. (2017) reported carbon-fixation rates of soil autotrophic microbes in wetland, grassland, and woodland soils to be 85.1, 21.9, and 32.9 mg C m^{-2} d^{-1}, respectively. Similarly, Huang et al. (2022) observed notable disparities in carbon-fixation rates between forest and grassland soils in the Loess Plateau. These findings underscore the influence of vegetation types on soil carbon-fixation rates, which are pivotal for projecting the carbon-fixation potential of soil autotrophic microbes in the red soil region. Nonetheless, the underlying mechanisms of this influence remain to be elucidated.

This study seeks to explore the dynamic shifts in CO_2 fixation rates by autotrophic microorganisms within the red soil region and to furnish a theoretical framework for appraising the carbon-fixation potential of microbes across terrestrial ecosystems in the red soil regions of China. We examined the distribution patterns of soil carbon content and the CO_2 fixation. Employing bacterial 16S rRNA high-throughput sequencing, real-time fluorescent quantitative PCR, and stable isotope labeling techniques, we quantified the CO_2 fixation capacities of soil autotrophic microorganisms under different vegetation types. Additionally, we delineated the characteristics of soil autotrophic microbial communities, and identified the key biotic and abiotic determinants influencing carbon fixation.

2 Methods

2.1 Sample collection and pre-treatment

The research site is situated at the Qianyanzhou Red Soil Hill Comprehensive Development Experimental Station in Jiangxi Province, China, which lies within the subtropical monsoon climate zone. The station experiences an average annual temperature of 17.9°C and receives an average annual precipitation of 1,475 mm. The predominant soil type is red soil, classified as ferralsols, originating from red sandstone and mudstone (Shao et al., 2009; Jiang et al., 2020; IUSS Working Group WRB, 2022; Zhou L. et al., 2024). For this study, soils from five vegetation types were selected: paddy fields (PS), orchards (OS), wastelands (WS), broad-leaved forests (BFS, primarily comprising *Liriodendron chinense, Liquidambar formosana Hance*, and *Cinnamomum camphora Presl*), and coniferous forests (CFS, chiefly consisting of *Cunninghamia lanceolata*, *Pinus elliottii Engelmann*, and *Pinus massoniana*) (Supplementary Figure S1). Following the methodology of Bao (2000), soil samples were collected from three strata: 0–10 cm, 10–30 cm, and 30–50 cm. Utilizing a soil drill and an S-type sampling scheme, five subsamples from each depth were mixed into a single composite sample. This process was replicated for three plots per vegetation type, with each plot separated by a minimum of 200 m, yielding a total of 45 soil samples. Post-homogenization, extraneous materials such as gravel and roots were excised, and the samples were sifted through a 2 mm sieve. Each sample was then bifurcated: one portion first immediately designated for DNA extraction and microbial sequencing, preserved at below −80°C ultra-low temperature refrigerator (DW-HL678D, Zhongke Meiling Cryogenic Technology Co., LTD., Hefei, Anhui, China); the other (remaining sample) reserved as the second part of the research material, air-dried and stored at 4°C refrigerator (BCD-539WT, Haier

Smart Home Co., LTD., Qingdao, Shandong, China) for subsequent analysis of soil physical and chemical attributes.

2.2 Soil physical and chemical properties analysis

The total iron (Fe) content and its various forms were quantified in 0.2 g of air-dried red soil, which had been passed through a 100-mesh sieve (100 openings per inch). Following the methodologies outlined by Jeewani et al. (2021), different forms of Fe were extracted from the soil samples: free iron oxide (Fe_d) using the sodium disulfite - sodium citrate - sodium bicarbonate method, amorphous iron oxide (Fe_a) with ammonium oxalate buffer solution, and complexed iron oxide (Fe_c) via sodium pyrophosphate solution. Total Fe was extracted by dissolving the soil in a mixture of 5 mL 8 M HNO_3, 2 mL 12 M HCl, and 2 mL HF. The Fe content in the extraction solution was determined using a flame atomic absorption spectrometer (200 series AA, Agilent, USA).

Soil organic carbon (SOC) was measured employing the external heating method with potassium dichromate. Microbial biomass carbon (MBC) and dissolved organic carbon (DOC) were extracted using the chloroform fumigation-K_2SO_4 method and a soil-water mixing procedure at a ratio of 1:5 followed by shaking centrifugation, respectively. The extracts were then analyzed by a total organic carbon analyzer (MultiC/N3100, Jena, Germany). Readily oxidized organic carbon (ROC) was assessed using the 333 mM $KMnO_4$ oxidation method. Soil pH was measured using soil-determination of pH-potentiometry method (HJ 962–2018, China) with a pH meter (FE28, Mettler Toledo, USA) at a soil-to-water ratio of 1:2.5. Total nitrogen (TN) and total phosphorus (TP) were quantified using an elemental analyzer (Vario Max CN, Elementar, Germany) and the molybdenum-antimony anti-spectrophotometric method, respectively.

2.3 Extraction and high-throughput sequencing of soil DNA

The samples were used for DNA isolation in triplicate. Total DNA was extracted from fresh soil samples utilizing the Power Soil™ Total DNA Isolation Kit (Qiagen, Hilden, Germany), and its concentration and purity were assessed using a NanoDrop nucleic acid quantifier (ND-1000, Thermo Scientific, USA) based on the absorbance ratios of A260/A280 and A260/A230. The DNA samples were subsequently stored at −80°C for future analysis. The carbon fixation functional microbial community was characterized using *cbbL* primers (K2f (5'-ACCAYCAAGCCSAAGCTSGG-3') and V2r (5'-GCCTTCS AGCTTGCCSACCRC-3')) and analyzed via the Illumina MiSeq high-throughput sequencing platform (Shanghai Majorbio Bio-Pharm Technology Co. Ltd., Shanghai, China) (Qin et al., 2021). Raw sequences underwent initial processing with Trimmomatic software for filtering and FLASTQ software for assembly. Subsequent quality control, de-noising, merging, and de-chimerization of all sequences were conducted using the DADA2 plug-in within Qiime 2 software. High-quality sequences were then clustered at a 97% similarity threshold into operational taxonomic units (OTUs). The most abundant sequence within each OTU was designated as the representative sequence, with a confidence threshold set at 0.7. Classification of bacterial 16S rRNA and *cbbL* gene sequences was performed against the silva138 and unite8.0 databases, respectively, to ascertain taxonomic information and relative abundance distributions (Tiquia et al., 2002).

2.4 Soil carbon fixation culture experiment

To initiate microbial carbon fixation activity, 50 g of dry soil samples, sieved through a 2 mm mesh, were placed into 500 mL conical flasks with rubber stoppers and pre-incubated under illumination at 25°C for 15 days (Ge et al., 2013). CO_2 was purged from the flasks by injecting a synthetic air mixture (75% N_2 and 25% O_2). Subsequently, the flasks containing soil samples were divided into two parallel sets. One set was injected with 0.2 mL of ^{13}C-labeled CO_2, while the control set received 0.2 mL of ^{12}C-CO_2. The CO_2 concentration within the flasks was maintained at approximately 400 ppm. A 40-day labeling experiment was conducted refer to previous studies (Miltner et al., 2005; Huang et al., 2022), during which air and $^{13}CO_2/^{12}CO_2$ were periodically reintroduced every 5 days to maintain oxygenation and constant isotope concentration. Concurrently, ultra-pure water was periodically added to each flask to compensate for soil water evaporation. The culture room temperature was regulated to 25 ± 1°C from 8 am to 8 pm daily, with artificial light intensity sustained at 0.5 mol photons m^{-2} s^{-1}; the temperature was adjusted to 15 ± 1°C from 8 pm to 8 am. Post-experimentation, soil samples were air-dried and sieved for ^{13}C-SOC content analysis. A 1.5 g air-dried sample was sifted through a 0.15 mm mesh, transferred to a 10 mL centrifuge tube, and treated with 3 mL of 2.5 mol L^{-1} HCl for 24 h to eliminate inorganic carbon. After centrifugation, the HCl was decanted, and the residue was rinsed twice with ultra-pure water to remove residual acid (Ge et al., 2013). The stable carbon isotope ratio ($^{13}C/C$) of the soil samples was determined via isotope ratio mass spectrometry (MAT253, Thermo Fisher Scientific, USA) following HCl treatment. The ^{13}C-SOC content and carbon-fixation rate (Rs) were calculated using Equations 1, 2 (Huang, 2021), respectively.

$$^{13}C - SOC = SOC \times \left[\left(AT\% \left(labeled \right) - AT\% \left(unlabeled \right) \right) \right] \times 10 \quad (1)$$

$$R_S = ^{13}CSOC1/S/T \quad (2)$$

AT% (labeled) signifies the proportion of microbial carbon-fixation isotope atoms present in labeled soil, whereas AT% (unlabeled) indicates the proportion of organic carbon isotope atoms in unlabeled soil. The carbon-fixation rate (Rs) is quantified in mg C kg^{-1} soil d^{-1}; ^{13}C-SOC denotes the ^{13}C-enriched soil organic carbon content, measured in mg kg^{-1}. The bottom area of the container (S), with a diameter of 0.05 m, is expressed in m^2; T denotes the duration of the experiment, which was conducted over a period of 40 days.

2.5 Data analysis

Data processing was conducted using Microsoft 365 Excel, statistical analysis was performed with IBM SPSS 19.0, and data

visualization was facilitated by Origin 2022. A one-way ANOVA, followed by the Least Significant Difference (LSD) test and Duncan's multiple range test (DMRT), was employed to discern significant differences in soil environmental factors and soil organic carbon composition across various treatments. The BioProjectID is PRJNA1174083 in SRA database. For the co-occurrence network analysis, only bacterial genera within the top 100 relative abundances were considered, with correlation coefficients exceeding an absolute value of 0.5 and p-values below 0.01 deemed statistically robust for network generation. Networks were visualized utilizing Gephi (Barberán et al., 2012), with node size reflecting the number of connections (degree), node color denoting major phyla, and edges indicating pairwise correlations.

Non-metric Multidimensional Scaling (NMDS) based on Bray–Curtis dissimilarity was executed to assess microbial community composition variances, while Analysis of Similarity (ANOSIM) tested the significance of microbial community differences between vegetation types ($n = 999$ permutations). A structural equation model elucidating the relationship between the Rs and soil autotrophic bacterial community, SOC, MBC, Fe, and pH was constructed using IBM SPSS Amos 25.0. In this model, the autotrophic bacterial community was represented by the Shannon index. The model underwent further refinement based on the algorithmic outcomes of the theoretical model, with a p-value greater than 0.05 in the chi-square test indicating a satisfactory fit with the data.

3 Results

3.1 Differences in physical and chemical properties of soil

The quantification of soil carbon components under various vegetation types revealed significant findings, as depicted in Figure 1. The CFS exhibited the highest SOC content in the surface layer (0–10 cm), registering at 18.11 g kg^{-1}, followed by PS at 15.80 g kg^{-1}, WS at 14.58 g kg^{-1}, BFS at 13.80 g kg^{-1}, and OS at 13.54 g kg^{-1}. The highest DOC and ROC contents in the surface layer were found in PS (118.01 mg kg^{-1}) and OS (2.06 g kg^{-1}), respectively, with the lowest values recorded in BFS (67.77 mg kg^{-1}) and CFS (1.41 g kg^{-1}). A trend of decreasing SOC, DOC, and ROC contents with increasing soil depth was observed across all vegetation types. MBC content showed a decrease with soil depth in PS and OS, whereas an increase was noted in WS, BFS, and CFS.

TP and TN contents, detailed in Supplementary Table S1, were highest in the surface layer of PS (0.62 g kg^{-1} and 1.93 g kg^{-1}, respectively) and exhibited a decline with increasing soil depth across all vegetation types. The soil layers from 0 to 30 cm in PS and OS demonstrated higher carbon, TP, and TN contents compared to WS. Soil pH levels were acidic across all sampling points, ranging from 4.57 to 6.27, with PS soils showing the highest pH values (5.11–6.27) and BFS soils the lowest (4.73–4.79). Furthermore, the contents of Fe$_c$, Fe$_a$, and Fe$_d$ varied between 0.68 to 2.90 g kg^{-1}, 0.39 to 2.51 g kg^{-1}, and 5.81 to 18.27 g kg^{-1} in Supplementary Table S1, respectively. No significant differences were observed among soil layers for Fe$_c$ and Fe$_a$ contents. The surface soil layer exhibited lower total Fe content compared to the deeper layers (10–50 cm) in all vegetation types, with the exception of WS.

3.2 $^{13}CO_2$ fixation rate of soil

Following a 40-day period of indoor cultivation, the ^{13}C-SOC content in the soil spanned from 0.75 to 3.21 mg kg^{-1}, as detailed in Supplementary Table S2. The ^{13}C-SOC content was found to be higher in the 0–10 cm layer compared to the 10–30 cm layer. The ratio of ^{13}C-SOC to SOC fluctuated between 0.012 and 0.039%, with the autotrophic carbon fixation contribution to SOC in the 10–30 cm layer being significantly greater than that in the 0–10 cm layer. The ^{13}C fixation rates across different vegetation types were ranked as follows: PS (0–10 cm, 18.15 mg C kg^{-1} soil d^{-1}; 10–30 cm, 16.71 mg C kg^{-1} soil d^{-1}) > OS > CFS > BFS > WS (0–10 cm, 9 mg C kg^{-1} soil d^{-1}; 10–30 cm, 4.25 mg C kg^{-1} soil d^{-1}). Additionally, the ^{13}C fixation rate in the 0–10 cm soil layer was consistently higher than that in the 10–30 cm soil layer for all vegetation types.

3.3 Community diversity of soil carbon-fixation microorganisms

OTU clustering analysis disclosed a range of 488 to 1,088 OTUs within the sampled soils, as depicted in Figure 2a. Notably, BFS demonstrated a significantly higher number of OTUs in comparison to PS, OS, and CFS. The diversity, evenness, and richness of soil microbial communities, influenced by varying vegetation types, were quantitatively evaluated using several indices: the Chao index for richness, the Simpson index for evenness, and the Shannon index for diversity, with their respective assessments illustrated in Figures 2b–d. The findings indicated that both the Shannon and Chao indices reached their peak values in BFS soil, while the lowest values were recorded in CFS soil. In contrast, the Simpson index was highest in PS soil and lowest in BFS soil. Following a multivariate stepwise regression analysis (Supplementary Table S3) to identify factors influencing carbon fixation rates, the explanation degree of Shannon index for the variability of the synthesis rate of ^{13}C-SOC was 67.07%, followed by SOC (35.23%), TP (8.8%), DOC (7.2%), the Simpson index (3.21%), and the Chao index (5.01%). The Shannon diversity index emerged as having the most substantial effect, and this observation is slated for further validation through Pearson correlation analysis.

3.4 Soil autotrophic microbial community composition and co-occurrence network

Within soil ecosystems, excluding unidentifiable entities, the dominant autotrophs are primarily represented by five bacterial groups: Proteobacteria, Actinobacteria, Armatimonadetes, Planctomycetes, and candidate_division_NC10. Collectively, these groups account for 78.2 to 90.1% of the total bacterial population, as illustrated in Figure 3a. The distribution of Proteobacteria is notably higher in CFS and BFS compared to PS, OS, and WS. In contrast, Actinobacteria exhibit an inverse pattern of relative abundance. At a finer taxonomic resolution, the top 30 autotrophic communities were analyzed, excluding unidentified groups. The genera *Bradyrhizobium*, *Azospirillum*, *Burkholderia*, *Paraburkholderia*, and *Thermomonospora* emerged as the most abundant, as depicted in Figure 3b. *Bradyrhizobium* was the most prevalent across various soil types, with
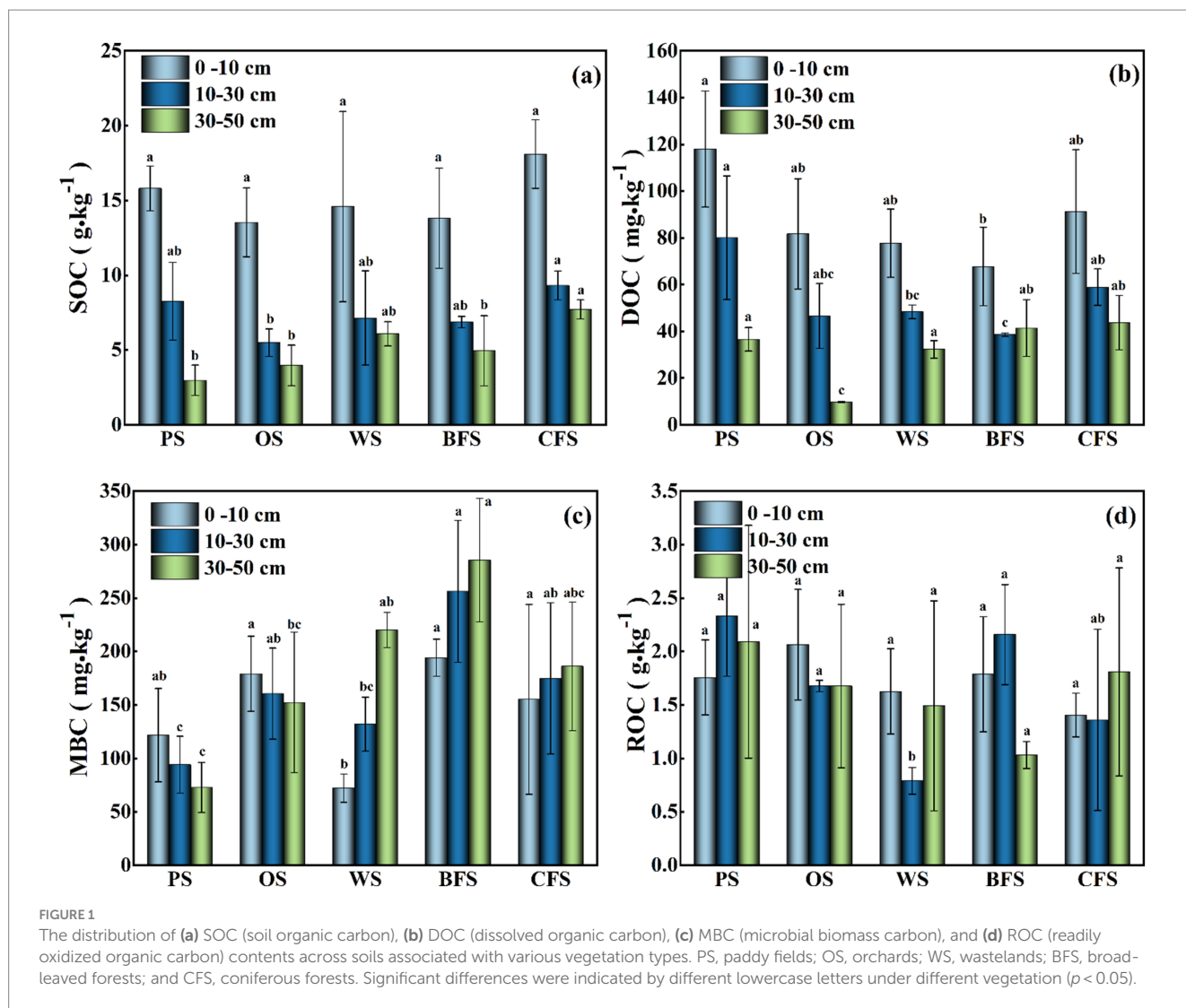
FIGURE 1

The distribution of **(a)** SOC (soil organic carbon), **(b)** DOC (dissolved organic carbon), **(c)** MBC (microbial biomass carbon), and **(d)** ROC (readily oxidized organic carbon) contents across soils associated with various vegetation types. PS, paddy fields; OS, orchards; WS, wastelands; BFS, broad-leaved forests; and CFS, coniferous forests. Significant differences were indicated by different lowercase letters under different vegetation ($p < 0.05$).

an abundance ranging from 16.1 to 30.0%. *Azospirillum* recorded its highest mutual abundance of 11.1% in CFS. *Paraburkholderia* demonstrated a lower relative abundance in PS, OS, and WS compared to BFS and CFS. Conversely, *Thermomonospora*'s relative abundance was found to be highest in PS, while it was lowest in BFS.

Non-metric Multidimensional Scaling (NMDS) was employed to discern the driving factors behind the disparities in microbial community structures. The analysis indicated a significant influence of vegetation type on microbial community composition (ANOSIM: R = 0.904, $p = 0.01$), as depicted in Figure 4a. Furthermore, Permutational Multivariate Analysis of Variance (PERMANOVA) attributed 65.72% of the variance to the impact of different vegetation types and 8.58% to soil depths on autotrophic microbial community composition, as detailed in Supplementary Table S5. Quantitative Polymerase Chain Reaction (qPCR) results demonstrated that the copies of *cbbL* functional genes in all vegetation soils spanned from 6.4×10^7 to 1.8×10^{10} copies g^{-1} fresh soil (Figure 4b). In PS, OS, and WS, the copies of *cbbL* functional genes diminished with increasing soil depth. Conversely, in BFS and CFS, the copies of *cbbL* functional genes escalated with soil depth, corroborating the ^{13}C fixation rate results presented in Supplementary Table S2.

Co-occurrence networks were generated to elucidate potential interactions among soil microorganisms across five vegetation types. The topological properties of these networks are illustrated in Figure 5. The collinear network associated with PS exhibited the highest edge density, with a network density quantified as 333 edges and a map density of 0.075. In contrast, WS demonstrated the lowest edge density. The average network width size followed the sequence: PS > CFS > WS > OS > BFS, as detailed in Supplementary Table S6.

3.5 Correlation between autotrophic microorganisms and environmental factors

Pearson correlation analysis (Figure 6) revealed that the soil carbon fixation rate (Rs) was significantly correlated with the Shannon index, TP, TN, DOC, Fe$_c$ and Fe$_a$ ($p < 0.05$). The Shannon index also showed significant correlations with Fe$_a$, Fe$_d$, TP, TN and DOC ($p < 0.05$). Additionally, the copies of the *cbbL* gene in soil was significantly correlated with pH ($p < 0.01$). The positive correlation between TP and Rs may be attributed to the role of essential phosphorous compounds in the carbon fixation pathways of
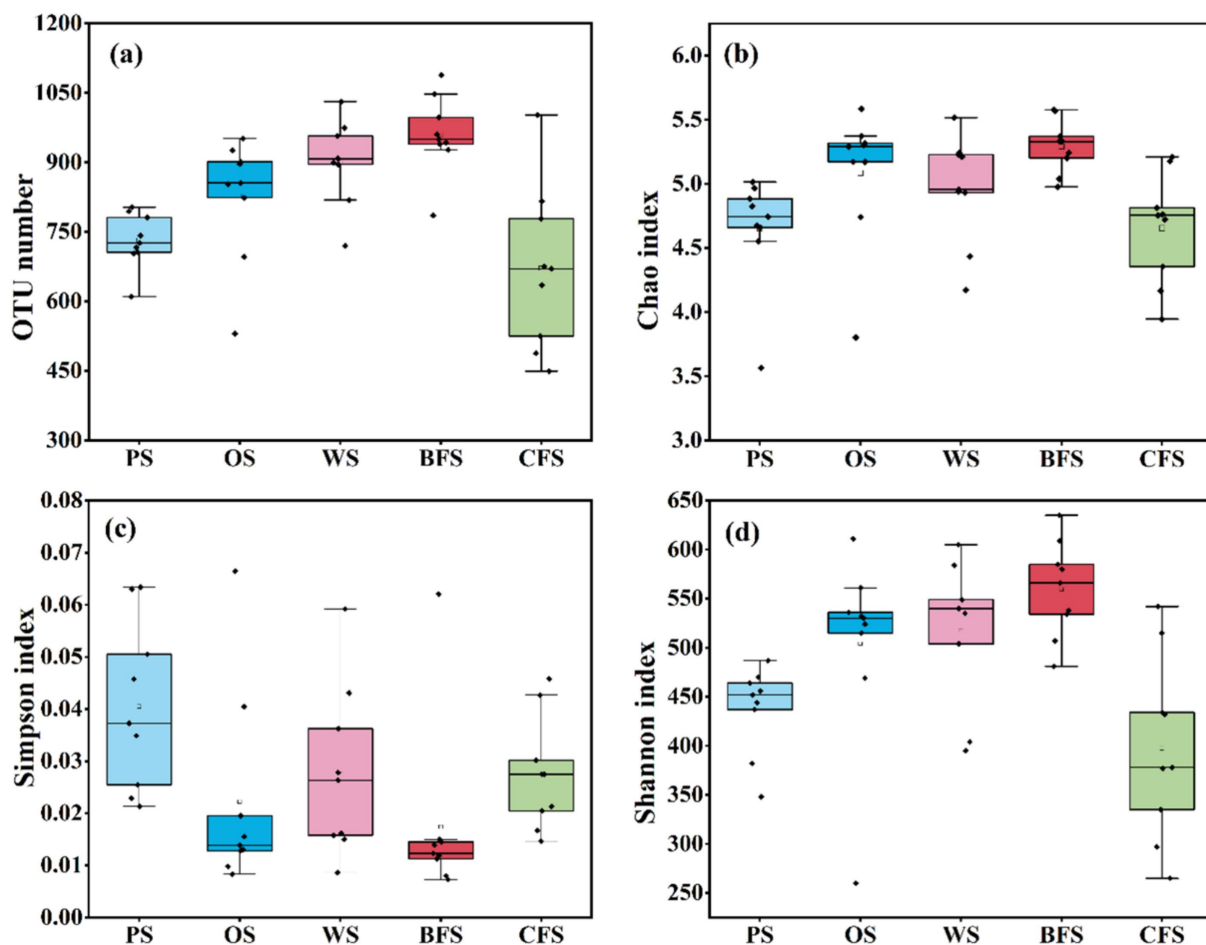
FIGURE 2
(a) OTU number, and (b) Chao, (c) Simpson, and (d) Shannon indices for soil microorganisms across different vegetation types. The sequencing data for microorganisms in various soil layers (0−10, 10−30, and 30−50 cm) are consolidated in the figure, with detailed information provided in Supplementary Table S4.
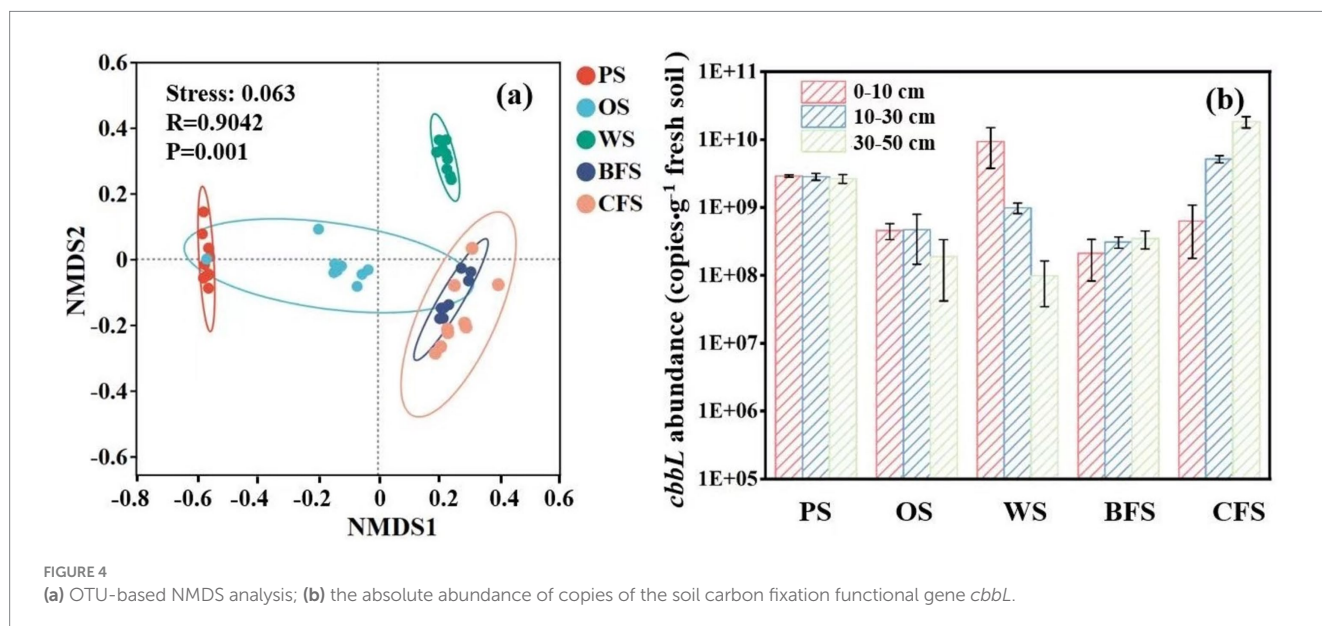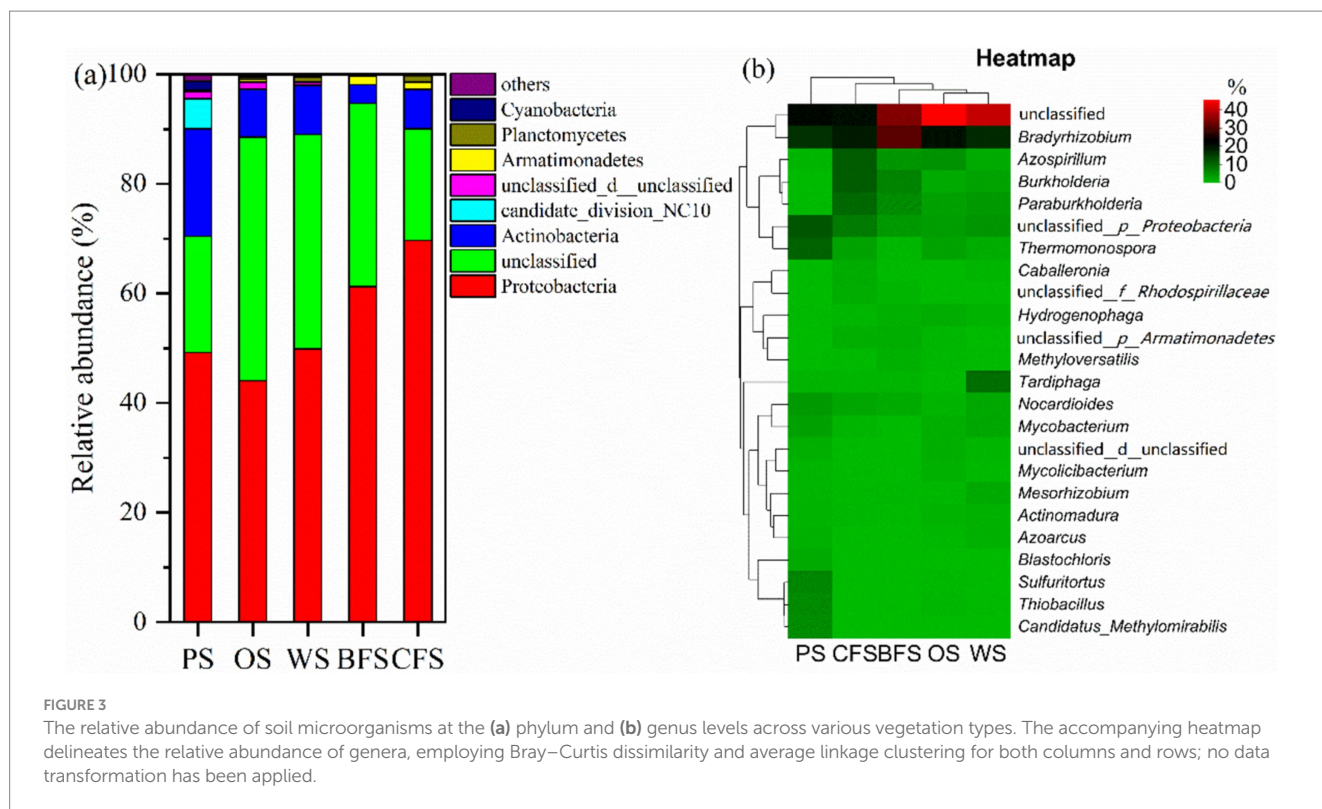
autotrophs, including heptose 7-phosphate and D-fructose 1,6-diphosphate in the Calvin cycle, as well as phosphoenolpyruvate in the rTCA and DC/4-HB cycles (Zheng Z. C. et al., 2022). Further Pearson correlation analysis suggested positive associations between SOC, the Shannon index, and Rs, indicating that SOC may enhance facultative autotrophic bacterial growth.

The structural equation model (SEM) further substantiated that Rs was influenced by SOC and autotrophs ($\chi 2 = 7.219$, df = 6, $p = 0.301$, RMSEA = 0.068, GFI = 0.952), as illustrated in Figure 7. The SEM elucidated that Fe indirectly affected the carbon fixation rate by modulating SOC, and pH indirectly impacted Rs by influencing the diversity of autotrophic microorganisms. Consequently, soil acidification may impede the carbon fixation function of bacterial communities (Li et al., 2021).

4 Discussion

The surface soil layer of PS and OS exhibited higher SOC, TP, and TN contents compared to other vegetation types, as indicated in Figure 1 and Supplementary Table S1. This disparity may be attributed

to the application of inorganic or organic fertilizers, which are rich in nitrogen and phosphorus, on agricultural lands (Hao et al., 2019; Zheng F. J. et al., 2022). Conversely, SOC, DOC, MBC, and TN contents in BFS and CFS were superior to those in WS and OS, which can be ascribed to the enhanced absorption of soil nutrients during plant growth in the initial stages of vegetation restoration in WS (Zhu et al., 2023). As a result, WS exhibited a lower nutrient content relative to other vegetation cover types. The elevated SOC content in BFS and CFS suggests that the input of forest litter may compensate for the nutrient depletion following plant uptake (Pan et al., 2023). However, the humic acid produced by litter decomposition could further reduce soil pH (Rahim et al., 2024). Additionally, the organic acids secreted by coniferous forests, such as *Cunninghamia lanceolat*, to solubilize and assimilate phosphorus from soil minerals, also contribute to the reduction in soil pH (Pan et al., 2023). The highest SOC content recorded in CFS surface soil (18.11 g kg^{-1}) might be correlated with the shallow root depth of conifers and the retention of easily degradable rhizosphere sediments within the topsoil (Yan et al., 2018; Duan P. P. et al., 2023). In contrast, broadleaf trees, which possess a higher root biomass, allocate more carbon from decomposable roots to deeper soil strata (Panchal et al., 2022), potentially explaining the

FIGURE 3
The relative abundance of soil microorganisms at the (a) phylum and (b) genus levels across various vegetation types. The accompanying heatmap delineates the relative abundance of genera, employing Bray–Curtis dissimilarity and average linkage clustering for both columns and rows; no data transformation has been applied.

FIGURE 4
(a) OTU-based NMDS analysis; (b) the absolute abundance of copies of the soil carbon fixation functional gene *cbbL*.
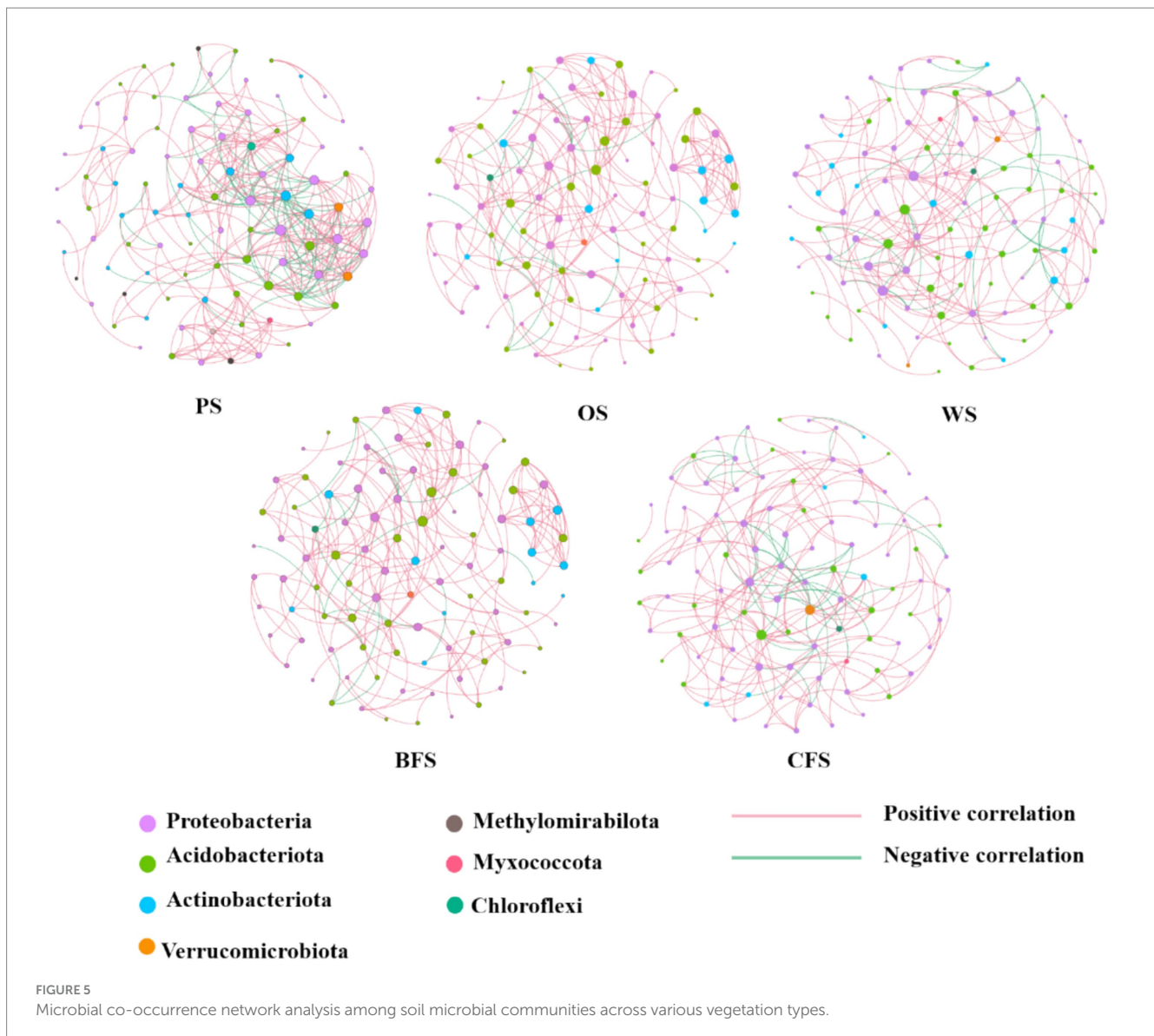
observed increase in MBC content in the deeper layer (0–50 cm) of BFS compared to CFS (Figure 1c).

Furthermore, iron plays a pivotal role in the fixation of soil organic carbon (Song et al., 2022). The forms of iron influence the accumulation and stability of soil carbon (Duan X. et al., 2023), where the interaction between iron minerals and organic matter may form an iron-soil organic carbon complex, potentially reducing the bioavailability of soil organic carbon to microorganisms (Herndon et al., 2017; Duan X. et al., 2023; Yang et al., 2023). This interaction may lead to enhanced carbon sequestration in deeper soils.

Augmenting the sequestration of soil organic carbon not only ameliorates soil quality and fertility but also contributes to a primary strategy for mitigating global climate change (Nazir et al., 2024).

Environmental factors such as temperature, land use, nutrient content, and soil depth are significant determinants of CO_2 fixation by soil autotrophs (Bhattacharyya et al., 2022; Zhang et al., 2023). Liao et al. (2020) investigated the differences in soil carbon fixation rates between chemically and organically fertilized farmlands, attributing the diminished CO_2 fixation rate in chemically fertilized soils to decreased soil pH and increased nutrient concentrations. Additionally,

FIGURE 5
Microbial co-occurrence network analysis among soil microbial communities across various vegetation types.

Li et al. (2021) posited that alterations in the soil carbon-to-nitrogen (C/N) ratio significantly affect the rate of soil microbial carbon fixation, likely due to the ratio's facilitation of microbial growth and metabolism, thus enhancing microbial carbon fixation processes. This study demonstrated that PS could sequester more CO_2, as shown in Supplementary Table S2, while farmland abandonment (wasteland) proved less conducive to soil carbon fixation. PS exhibited a higher rate of carbon fixation compared to other soil types, albeit lower than the CO_2 fixation rate of Tibetan Plateau soil ($18–29\,mg\,C\,kg^{-1}$ soil d^{-1}) reported by Zhao et al. (2018). Prior research indicates that paddy field soil harbors a larger fraction of obligate autotrophic bacteria and exhibits greater ribulose-1,5-bisphosphate carboxylase/oxygenase (RubisCo) enzyme activity, with its CO_2 fixation rate being four times that of dryland and forest soils (Lynn et al., 2017; Liao et al., 2020). Numerous studies support the critical role of SOC in modulating carbon fixation rates (Bu et al., 2023), with variations in unstable soil organic matter altering the composition of the autotrophic bacterial community—specifically, the balance between obligate and facultative autotrophs—and thereby influencing microbial carbon fixation potential (Badger and Bek, 2008). Moreover, Fe_c and Fe_a are

significantly correlated with the Rs and positively associated with SOC (Figure 6). Fe_c is likely to form complexes with simple SOC and organic acids via coordination bonds (Rezapour et al., 2015), while iron ions may act as electron acceptors for extrinsic iron reduction, affecting carbon fixation within autotrophic bacterial communities (Liu et al., 2019). The Spearman correlation heatmap (Figure 8) demonstrated that eight dominant bacterial species containing the *cbbL* gene were significantly correlated with pH value ($p < 0.05$), likely due to the sensitivity of soil microorganisms, particularly bacteria, to changes in soil pH (Fierer et al., 2007; Raniolo et al., 2023). Moreover, Fe, Fe_c and Fe_a showed significant correlations with dominant microbial genera ($p < 0.05$). Spearman correlation analysis also revealed significant correlations of TP with *Mycolicibacterium*, *Sulfitobacter*, *Thiobacillus*, and *Thermomonospora*. A global meta-analysis demonstrated that soil pH influences bacterial composition more strongly than spatial or climatic factors (biomes). Furthermore, an analysis of 942 soil bacterial genera found that only 0.8% were tolerant of low pH, whereas 21% were tolerant of high pH. Genera with an acidic pH optimum were more prevalent in humid climates (e.g., boreal forests, and tropical forests) (Zhou X. et al., 2024).
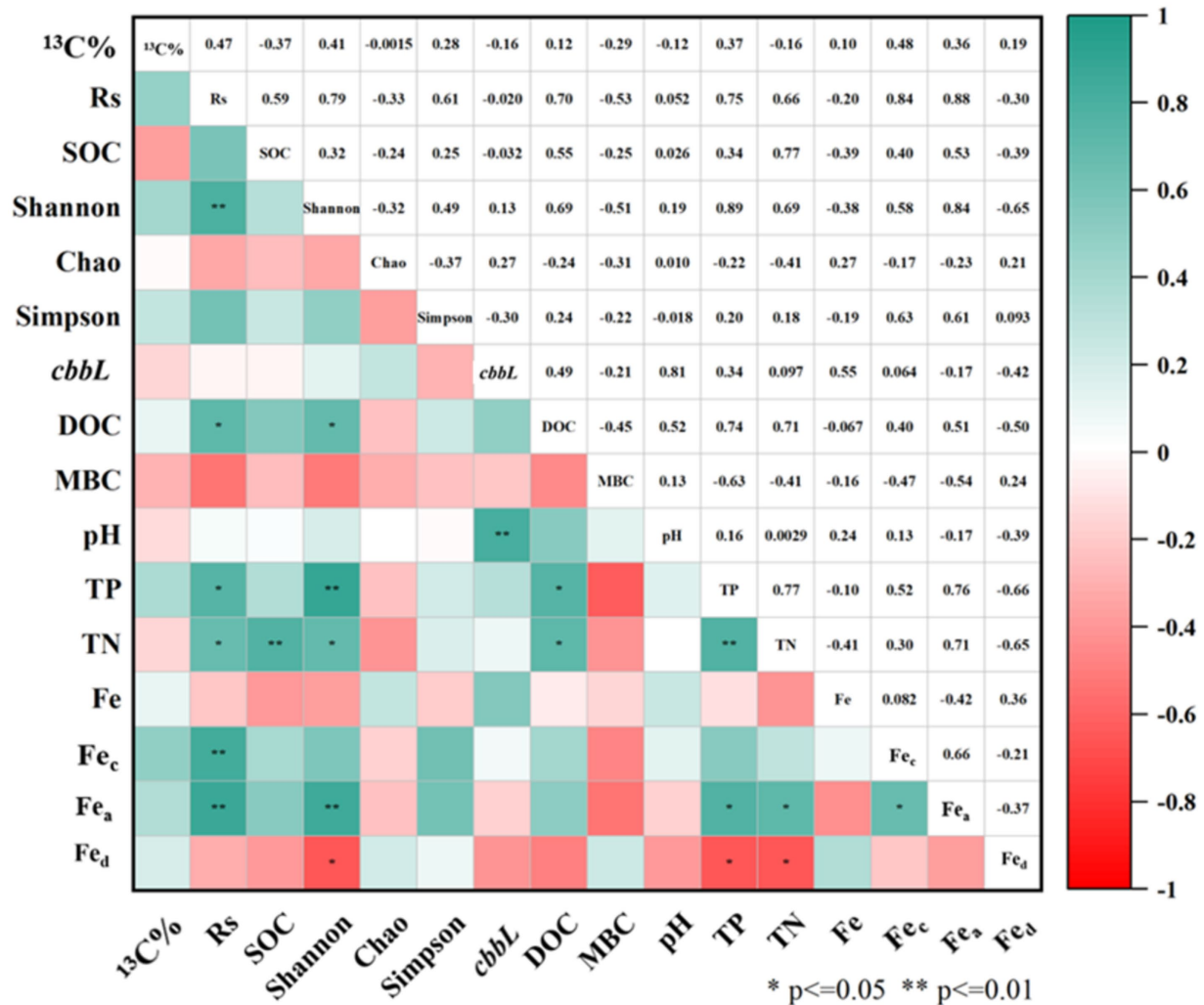
FIGURE 6
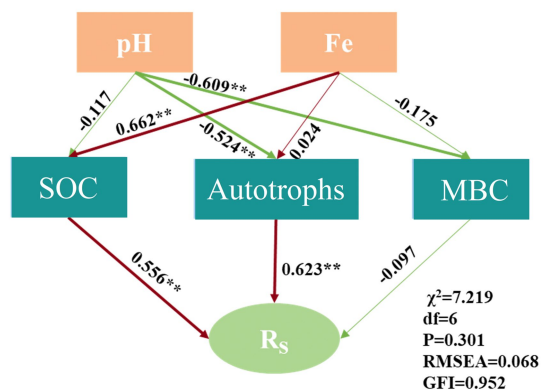Pearson correlation analysis matrix of soil physicochemical and community diversity parameters.

FIGURE 7
Structural equation model of factors influencing the carbon fixation rate.

Soil microorganisms play a pivotal role in regulating the carbon budget balance at the soil-atmosphere interface through the assimilation of CO_2 and the mineralization and decomposition of soil

organic matter (Tao et al., 2023; Ding et al., 2024; Wu et al., 2024; Yang et al., 2024). It is commonly posited by researchers that CO_2 fixation by soil autotrophic microorganisms predominantly occurs at the surface soil-atmosphere interface, leading to a frequent underestimation of the carbon fixation capacity of soil due to the overlooked contribution of deep soil microorganisms (Liao et al., 2023). An observed weak negative correlation between the abundance of the *cbbL* gene across various soil types and their CO_2 fixation capacity (Figure 4 and Supplementary Table S2) contrasts with findings by Li et al. (2021), who reported a positive correlation between the *cbbL* gene abundance and carbon fixation rates in the Tibetan Plateau and southern red soils. In contrast, Xiao et al. (2018) found no significant association between CO_2 fixation capabilities and *cbbL* gene abundance in erosive watershed and agricultural soils. This variance may be ascribed to the differing carbon assimilation potentials and metabolic strategies of autotrophs within the soil, as the abundance of autotrophic bacteria does not consistently correlate with CO_2 assimilation rates (Saini et al., 2011). Multiple linear regression analysis has identified SOC content and the Shannon index as the primary factors explaining variations in microbial carbon fixation rates (Supplementary Table S3). While previous research has indicated that alterations in tillage methods and vegetation succession can
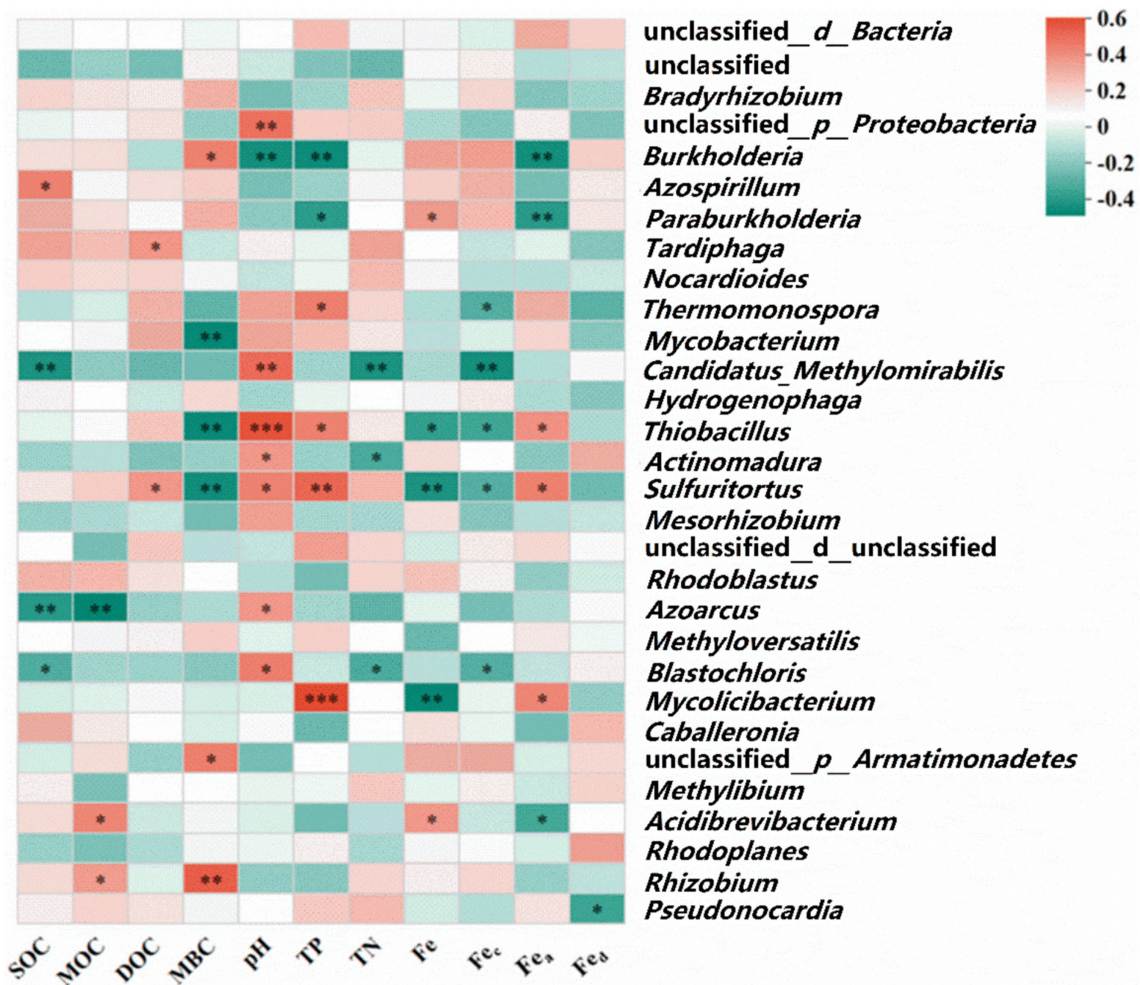
FIGURE 8
Spearman correlation analysis heatmap between the dominant genus and various environmental factors.

diminish microbial community diversity, the contrasting findings regarding community diversity in this study (Supplementary Table S4) may be attributed to the distinct influences exerted by different vegetation types on microbial populations (Zhao et al., 2019; Ramírez et al., 2020; Schmidt et al., 2021).

Obligate and facultative autotrophic bacteria are ubiquitous across all five vegetation types of soil. Certain microbial communities, including Proteobacteria, Actinobacteria, Armatimonadetes, and Planctomycetes, are recognized for their CO_2 fixation capabilities, as documented in previous studies (Vlaeminck et al., 2011; He et al., 2015; Bhattacharyya et al., 2022). The composition of carbon-fixing bacterial communities is known to vary across ecosystems; for instance, *Rhodopseudomonas palustris*, *Bradyrhizobium*, and *Ralstonia eutropha* are identified as predominant carbon fixation genera in wetlands (Lynn et al., 2017), while *Sulfuritalea*, *Ferriphaselus*, and *Thiohalorhabdus* dominate in karst region soils (Wang et al., 2021). The distinctive iron-rich and acidic conditions of the southern red soil region foster a unique carbon fixation bacterial community (Xing et al., 2022). Microbial co-occurrence network analysis has revealed the development and interactions within ecological niches, such as symbiosis, competition,

and predation (Barberán et al., 2012; Hu et al., 2022), as depicted in Figure 5. PS microorganisms exhibit the most intricate co-occurrence network, suggesting that ecosystems with higher nutrient content possess enhanced stability and versatility (Wagg et al., 2019). Conversely, in barren ecosystems, oligotrophic species predominate with minimal predation competition, resulting in weaker interaction relationships. The co-occurrence network displays strong positive correlations and few negative correlations, indicating potential cooperation among microbes to adapt to similar niches (Liang et al., 2017). Facultative bacteria such as *Bradyrhizobium* and *Mesorhizobium* demonstrate versatile capabilities, thriving autotrophically via the Calvin cycle and utilizing energy from inorganic sources like nitrogen, sulfur compounds, and iron oxides (Selesi et al., 2005; Wang et al., 2021). *Thiobacillus* species, for example, are known to use organic substrates as electron donors and Fe as electron acceptors, facilitating dissimilatory Fe reduction, which enhances the microbial carbon utilization rate and strengthens the soil carbon reservoir by increasing the microbial carbon fraction content within the entombing effect (Liang et al., 2017; Yao Y. et al., 2023). Additionally, *Odoricaulis* and *Methylibium* participate in sulfur oxidation processes, while *Bradyrhizobium* forms symbiotic

relationships with legumes, contributing to soil organic matter enhancement (Wang et al., 2021).

5 Conclusion

This study highlights the intricate interplay between soil carbon dynamics, microbial activity, and environmental factors in red soil ecosystems. The pronounced vertical variation in soil carbon content, which was more significant than horizontal distribution. The carbon fixation rate distribution revealed that PS exhibited nearly twice the fixation rate of WS, underscoring the important role of vegetation type in influencing carbon fixation. Both the Shannon index and SOC were key factors explaining the variability in soil carbon fixation rates across vegetation types. The results indicate that Fe and pH levels modulate carbon fixation by affecting SOC and the diversity of autotrophic bacterial communities. Although autotrophic carbon fixation contributed only 0.012 to 0.039% of total organic carbon within 40 days, its higher contribution in deeper soil layers emphasizes the importance of autotrophic carbon fixation in soils with low nutrient availability. Further research is needed to elucidate the mechanisms by which iron ions mediate microbial carbon fixation and facilitate the formation of stable carbon pools. These findings also have practical implications for sustainable agriculture and soil management. Targeted interventions, such as iron supplementation or pH regulation, could enhance microbial communities and improve carbon fixation. Additionally, this research supports the development of bio-based technologies, including microbial inoculants, to promote carbon storage and mitigate CO_2 emissions. A comprehensive understanding of microbial processes under different environmental conditions can inform the restoration of degraded red soils and guide climate mitigation strategies through improved soil carbon management. Advanced molecular tools—such as biomarker analysis, metagenomics combined with DNA-stable isotope probing, transcriptomics, and proteomics—will be crucial for identifying the specific microbial processes driving carbon fixation under both controlled and natural conditions. This research can provide a view for understanding the dynamic changes in microbial autotrophic CO_2 fixation rates in the red soil regions of China.

Data availability statement

The original contributions presented in the study are publicly available. This data can be found here: https://www.ncbi.nlm.nih.gov/bioproject/PRJNA1174083/BioProjectIDPRJNA1174083.

Author contributions

CL: Conceptualization, Data curation, Investigation, Methodology, Software, Validation, Writing – original draft. ZL: Conceptualization, Funding acquisition, Supervision, Validation, Writing – review & editing. RL: Investigation, Supervision, Writing – review & editing. LY: Investigation, Methodology, Writing – review & editing. FT: Data curation, Writing – review & editing. YW: Conceptualization, Data curation, Funding acquisition, Software, Writing – original draft, Writing – review & editing. GH: Conceptualization, Funding acquisition, Methodology, Supervision, Writing – original draft, Writing – review & editing.

Conflict of interest

The authors declare that they have no known competing financial interests or personal relationships that could have appeared to influence the work reported in this paper.

Publisher's note

All claims expressed in this article are solely those of the authors and do not necessarily represent those of their affiliated organizations, or those of the publisher, the editors and the reviewers. Any product that may be evaluated in this article, or claim that may be made by its manufacturer, is not guaranteed or endorsed by the publisher.

Supplementary material

The Supplementary material for this article can be found online at: https://www.frontiersin.org/articles/10.3389/fmicb.2024.1480484/full#supplementary-material

References

Anikwe, M., and Ife, K. (2023). The role of soil ecosystem services in the circular bioeconomy. *Front. Soil Sci.* 3:1209100. doi: 10.3389/fsoil.2023.1209100

Badger, M. R., and Bek, E. J. (2008). Multiple Rubisco forms in proteobacteria: their functional significance in relation to CO_2 acquisition by the CBB cycle. *J. Exp. Bot.* 59, 1525–1541. doi: 10.1093/jxb/erm297

Bahadori, M., Chen, C. R., Lewis, S., Boyd, S., Rashti, M. R., Esfandbod, M., et al. (2021). Soil organic matter formation is controlled by the chemistry and bioavailability of organic carbon inputs across different land uses. *Sci. Total Environ.* 770:145307. doi: 10.1016/j.scitotenv.2021.145307

Banerjee, S., Schlaeppi, K., and Van Der Heijden, M. G. A. (2018). Keystone taxa as drivers of microbiome structure and functioning. *Nat. Rev. Microbiol.* 16, 567–576. doi: 10.1038/s41579-018-0024-1

Bao, S. D. (2000). Agrochemical analysis of soil. *3rd* Edn. Beijing, China: China Agriculture Press.

Barberán, A., Bates, S. T., Casamayor, E. O., and Fierer, N. (2012). Using network analysis to explore co-occurrence patterns in soil microbial communities. *ISME J.* 6, 343–351. doi: 10.1038/ismej.2011.119

Bhattacharyya, S. S., Ros, G. H., Furtak, K., Iqbal, H. M. N., and Parra-Saldívar, R. (2022). Soil carbon sequestration – An interplay between soil microbial community and soil organic matter dynamics. *Sci. Total Environ.* 815:152928. doi: 10.1016/j.scitotenv.2022.152928

Bossio, D. A., Cook-Patton, S. C., Ellis, P. W., Fargione, J., Sanderman, J., Smith, P., et al. (2020). The role of soil carbon in natural climate solutions. *Nat. Sustain.* 3, 391–398. doi: 10.1038/s41893-020-0491-z

Bu, L. Y., Peng, Z. H., Tian, J., Zhang, X. X., Chen, W. F., An, D. R., et al. (2023). Core autotrophic microbes drive functional stability of soil *cbbL*-containing autotrophic microbes during desertification. *Appl. Soil Ecol.* 190:105027. doi: 10.1016/j.apsoil.2023.105027

Cheng, H. T., Zhou, X. H., Dong, R. S., Wang, X. M., Liu, G. D., and Li, Q. F. (2023). Natural vegetation regeneration facilitated soil organic carbon sequestration and microbial community stability in the degraded karst ecosystem. *Catena* 222:106856. doi: 10.1016/j.catena.2022.106856

Chu, H. Y., Sun, H. B., Tripathi, B. M., Adams, J. M., Huang, R., Zhang, Y. J., et al. (2016). Bacterial community dissimilarity between the surface and subsurface soils equals horizontal differences over several kilometers in the western Tibetan plateau. *Environ. Microbiol.* 18, 1523–1533. doi: 10.1111/1462-2920.13236

Ding, K., Chen, L. Y., Zhang, Y. T., Ge, S. Y., Zhang, Y. M., Lu, M., et al. (2024). Long-term cover crops boost multi-nutrient cycling and subsurface soil carbon sequestration by alleviating microbial carbon limitation in a subtropical forest. *Catena* 244:108252. doi: 10.1016/j.catena.2024.108252

Duan, P. P., Fu, R. T., Nottingham, A. T., Domeignoz-Horta, L. A., Yang, X. Y., Du, H., et al. (2023). Tree species diversity increases soil microbial carbon use efficiency in a subtropical forest. *Glob. Chang. Biol.* 29, 7131–7144. doi: 10.1111/gcb.16971

Duan, X., Li, Z., Li, Y. H., Yuan, H. Z., Gao, W., Chen, X. B., et al. (2023). Iron–organic carbon associations stimulate carbon accumulation in paddy soils by decreasing soil organic carbon priming. *Soil Biol. Biochem.* 179:108972. doi: 10.1016/j.soilbio.2023.108972

Fierer, N., Bradford, M. A., and Jackson, R. B. (2007). Toward an ecological classification of soil bacteria. *Ecology* 88, 1354–1364. doi: 10.1890/05-1839

Ge, T. D., Wu, X. H., Chen, X. J., Yuan, H. Z., Zou, Z. Y., Li, B. Z., et al. (2013). Microbial phototrophic fixation of atmospheric CO_2 in China subtropical upland and paddy soils. *Geochim. Cosmochim. Acta* 113, 70–78. doi: 10.1016/j.gca.2013.03.020

Hao, M. M., Hu, H. Y., Liu, Z., Dong, Q. L., Sun, K., Feng, Y. P., et al. (2019). Shifts in microbial community and carbon sequestration in farmland soil under long-term conservation tillage and straw returning. *Appl. Soil Ecol.* 136, 43–54. doi: 10.1016/j.apsoil.2018.12.016

He, S., Malfatti Stephanie, A., Mcfarland Jack, W., Anderson Frank, E., Pati, A., Huntemann, M., et al. (2015). Patterns in wetland microbial community composition and functional gene repertoire associated with methane emissions. *MBio* 6, e00066–e00015. doi: 10.1128/mbio.00066-15

Herndon, E., Albashaireh, A., Singer, D., Roy Chowdhury, T., Gu, B., and Graham, D. (2017). Influence of iron redox cycling on organo-mineral associations in Arctic tundra soil. *Geochim. Cosmochim. Acta* 207, 210–231. doi: 10.1016/j.gca.2017.02.034

Hu, L. N., Li, Q., Yan, J. H., Liu, C., and Zhong, J. X. (2022). Vegetation restoration facilitates belowground microbial network complexity and recalcitrant soil organic carbon storage in Southwest China karst region. *Sci. Total Environ.* 820:153137. doi: 10.1016/j.scitotenv.2022.153137

Huang, Q. (2021). The mechanism of CO_2 fixation by soil carbon-fixation microorganisms in the loess plateau. Yangling, Shanxi: Northwest A&F University.

Huang, Q., Huang, Y. M., Wang, B. R., Dippold, M. A., Li, H. H., Li, N., et al. (2022). Metabolic pathways of CO_2 fixing microorganisms determined C-fixation rates in grassland soils along the precipitation gradient. *Soil Biol. Biochem.* 172:108764. doi: 10.1016/j.soilbio.2022.108764

Huang, G. Q., and Zhao, Q. G. (2014). Initial exploration of red soil ecology. *Acta Ecol. Sin.* 34, 5173–5181. doi: 10.5846/stxb201405100944

IUSS Working Group WRB (2022). World Reference Base for soil resources (4th edition). International soil classification system for naming soils and creating legends for soil maps. Vienna, Austria: International Union of Soil Sciences.

Jeewani, P. H., Van Zwieten, L., Zhu, Z. K., Ge, T. D., Guggenberger, G., Luo, Y., et al. (2021). Abiotic and biotic regulation on carbon mineralization and stabilization in paddy soils along iron oxide gradients. *Soil Biol. Biochem.* 160:108312. doi: 10.1016/j.soilbio.2021.108312

Jiang, P. P., Meinzer, F. C., Wang, H., Kou, L., Dai, X. Q., and Fu, X. L. (2020). Below-ground determinants and ecological implications of shrub species' degree of isohydry in subtropical pine plantations. *New Phytol.* 226, 1656–1666. doi: 10.1111/nph.16502

Li, Y. C., Liang, X., Tang, C. X., Li, Y. F., Chen, Z. H., Chang, S. X., et al. (2018). Moso bamboo invasion into broadleaf forests is associated with greater abundance and activity of soil autotrophic bacteria. *Plant Soil* 428, 163–177. doi: 10.1007/s11104-018-3648-z

Li, Z. W., Tong, D., Nie, X. D., Xiao, H. B., Jiao, P. P., Jiang, J. Y., et al. (2021). New insight into soil carbon fixation rate: the intensive co-occurrence network of autotrophic bacteria increases the carbon fixation rate in depositional sites. *Agric. Ecosyst. Environ.* 320:107579. doi: 10.1016/j.agee.2021.107579

Li, Z. K., Xin, X. Q., Xiong, B., Zhao, D. D., Zhang, X. L., and Bi, C. H. (2020). Engineering the Calvin–Benson–Bassham cycle and hydrogen utilization pathway of *Ralstonia eutropha* for improved autotrophic growth and polyhydroxybutyrate production. *Microb. Cell Factories* 19:228. doi: 10.1186/s12934-020-01494-y

Liang, C., Schimel, J. P., and Jastrow, J. D. (2017). The importance of anabolism in microbial control over soil carbon storage. *Nat. Microbiol.* 2:17105. doi: 10.1038/nmicrobiol.2017.105

Liao, Q. H., Lu, C., Yuan, F., Fan, Q. Y., Chen, H. Y., Yang, L., et al. (2023). Soil carbon-fixing bacterial communities respond to plant community change in coastal salt marsh wetlands. *Appl. Soil Ecol.* 189:104918. doi: 10.1016/j.apsoil.2023.104918

Liao, H., Qin, F., Wang, K., Zhang, Y. C., Hao, X. L., Chen, W. L., et al. (2020). Long-term chemical fertilization-driving changes in soil autotrophic microbial community depresses soil CO_2 fixation in a Mollisol. *Sci. Total Environ.* 748:141317. doi: 10.1016/j.scitotenv.2020.141317

Liu, Y. L., Dong, Y. Q., Ge, T. D., Hussain, Q., Wang, P., Wang, J. K., et al. (2019). Impact of prolonged rice cultivation on coupling relationship among C, Fe, and Fe-reducing bacteria over a 1000-year paddy soil chronosequence. *Biol. Fertil. Soils* 55, 589–602. doi: 10.1007/s00374-019-01370-x

Lynn, T. M., Ge, T. D., Yuan, H. Z., Wei, X. M., Wu, X. H., Xiao, K. Q., et al. (2017). Soil carbon-fixation rates and associated bacterial diversity and abundance in three natural ecosystems. *Microb. Ecol.* 73, 645–657. doi: 10.1007/s00248-016-0890-x

Mason, A. R. G., Salomon, M. J., Lowe, A. J., and Cavagnaro, T. R. (2023). Microbial solutions to soil carbon sequestration. *J. Clean. Prod.* 417:137993. doi: 10.1016/j.jclepro.2023.137993

Miltner, A., Kopinke, F.-D., Kindler, R., Selesi, D., Hartmann, A., and Kästner, M. (2005). Non-phototrophic CO_2 fixation by soil microorganisms. *Plant Soil* 269, 193–203. doi: 10.1007/s11104-004-0483-1

Moore, O. W., Curti, L., Woulds, C., Bradley, J. A., Babakhani, P., Mills, B. J. W., et al. (2023). Long-term organic carbon preservation enhanced by iron and manganese. *Nature* 621, 312–317. doi: 10.1038/s41586-023-06325-9

Mukasa Mugerwa, T. T., and Mcgee, P. A. (2017). Potential effect of melanised endophytic fungi on levels of organic carbon within an Alfisol. *Soil Res.* 55, 245–252. doi: 10.1071/SR16006

Nazir, M. J., Li, G., Nazir, M. M., Zulfiqar, F., Siddique, K. H. M., Iqbal, B., et al. (2024). Harnessing soil carbon sequestration to address climate change challenges in agriculture. *Soil Tillage Res.* 237:105959. doi: 10.1016/j.still.2023.105959

Pan, C., Yu, W. R. N., Sun, C. C., Guo, J. H., Yu, Y. C., and Li, X. G. (2023). Saprotrophic fungi buffer the adverse effects of soil acidification on the soil nutrient supply ability of Chinese fir (*Cunninghamia lanceolata*) plantations. *Eur. J. Soil Biol.* 114:103462. doi: 10.1016/j.ejsobi.2022.103462

Panchal, P., Preece, C., Peñuelas, J., and Giri, J. (2022). Soil carbon sequestration by root exudates. *Trends Plant Sci.* 27, 749–757. doi: 10.1016/j.tplants.2022.04.009

Qin, J., Li, M., Zhang, H. F., Liu, H. M., Zhao, J. N., and Yang, D. L. (2021). Nitrogen deposition reduces the diversity and abundance of *cbbL* gene-containing CO_2-fixing microorganisms in the soil of the stipa baicalensis steppe. *Front. Microbiol.* 12:570908. doi: 10.3389/fmicb.2021.570908

Rahim, H. U., Allevato, E., Vaccari, F. P., and Stazi, S. R. (2024). Biochar aged or combined with humic substances: fabrication and implications for sustainable agriculture and environment-a review. *J. Soils Sediments* 24, 139–162. doi: 10.1007/s11368-023-03644-2

Ramírez, P. B., Fuentes-Alburquenque, S., Díez, B., Vargas, I., and Bonilla, C. A. (2020). Soil microbial community responses to labile organic carbon fractions in relation to soil type and land use along a climate gradient. *Soil Biol. Biochem.* 141:107692. doi: 10.1016/j.soilbio.2019.107692

Raniolo, S., Maretto, L., Benedetti Del Rio, E., Cournut, S., Cremilleux, M., Nowak, B., et al. (2023). Soil pH dominance over livestock management in determining bacterial assemblages through a latitudinal gradient of European meadows and pastures. *Ecol. Indic.* 155:111063. doi: 10.1016/j.ecolind.2023.111063

Rezapour, S., Azhah, H., Momtaz, H. R., and Ghaemian, N. (2015). Changes in forms and distribution pattern of soil iron oxides due to long-term cropping in the northwest of Iran. *Environ. Earth Sci.* 73, 7275–7286. doi: 10.1007/s12665-014-3933-y

Saini, R., Kapoor, R., Kumar, R., Siddiqi, T. O., and Kumar, A. (2011). CO_2 utilizing microbes — a comprehensive review. *Biotechnol. Adv.* 29, 949–960. doi: 10.1016/j.biotechadv.2011.08.009

Sanderman, J., Hengl, T., and Fiske, G. J. (2017). Soil carbon debt of 12,000 years of human land use. *Proc. Natl. Acad. Sci.* 114, 9575–9580. doi: 10.1073/pnas.1706103114

Schmidt, A., Hines, J., Türke, M., Buscot, F., Schädler, M., Weigelt, A., et al. (2021). The iDiv Ecotron—a flexible research platform for multitrophic biodiversity research. *Ecol. Evol.* 11, 15174–15190. doi: 10.1002/ece3.8198

Selesi, D., Schmid, M., and Hartmann, A. (2005). Diversity of green-like and red-like ribulose-1,5-bisphosphate carboxylase/oxygenase large-subunit genes (*cbbL*) in differently managed agricultural soils. *Appl. Environ. Microbiol.* 71, 175–184. doi: 10.1128/AEM.71.1.175-184.2005

Shao, Q. Q., Huang, L., Liu, J. Y., Yang, H. J., and Chen, Z. Q. (2009). Dynamic analysis on carbon accumulation of a plantation in Qianyanzhou based on tree ring data. *J. Geogr. Sci.* 19, 691–706. doi: 10.1007/s11442-009-0691-y

Song, X. X., Wang, P., Van Zwieten, L., Bolan, N., Wang, H. L., Li, X. M., et al. (2022). Towards a better understanding of the role of Fe cycling in soil for carbon stabilization and degradation. *Carbon Res.* 1:5. doi: 10.1007/s44246-022-00008-2

Spohn, M., Bagchi, S., Biederman, L. A., Borer, E. T., Bråthen, K. A., Bugalho, M. N., et al. (2023). The positive effect of plant diversity on soil carbon depends on climate. *Nat. Commun.* 14:6624. doi: 10.1038/s41467-023-42340-0

Sun, Y. X., Wang, X., Zhang, Y. Y., Duan, W. H., Xia, J. Y., Wu, J. H., et al. (2024). Vegetation types can affect soil organic carbon and $^\delta$13C by influencing plant inputs in topsoil and microbial residue carbon composition in subsoil. *Sustain. For.* 16:4538. doi: 10.3390/su16114538

Tao, F., Huang, Y. Y., Hungate, B. A., Manzoni, S., Frey, S. D., Schmidt, M. W. I., et al. (2023). Microbial carbon use efficiency promotes global soil carbon storage. *Nature* 618, 981–985. doi: 10.1038/s41586-023-06042-3

Tiquia, S. M., Lloyd, J., Herms, D. A., Hoitink, H. A. J., and Michel, F. C. (2002). Effects of mulching and fertilization on soil nutrients, microbial activity and rhizosphere bacterial community structure determined by analysis of TRFLPs of PCR-amplified 16S rRNA genes. *Appl. Soil Ecol.* 21, 31–48. doi: 10.1016/S0929-1393(02)00040-9

Vlaeminck, S. E., Hay, A. G., Maignien, L., and Verstraete, W. (2011). In quest of the nitrogen oxidizing prokaryotes of the early earth. *Environ. Microbiol.* 13, 283–295. doi: 10.1111/j.1462-2920.2010.02345.x

Wagg, C., Schlaeppi, K., Banerjee, S., Kuramae, E. E., and Van Der Heijden, M. G. A. (2019). Fungal-bacterial diversity and microbiome complexity predict ecosystem functioning. *Nat. Commun.* 10:4841. doi: 10.1038/s41467-019-12798-y

Wang, X. Y., Li, W., Xiao, Y. T., Cheng, A. Q., Shen, T. M., Zhu, M., et al. (2021). Abundance and diversity of carbon-fixing bacterial communities in karst wetland soil ecosystems. *Catena* 204:105418. doi: 10.1016/j.catena.2021.105418

Wu, H. W., Cui, H. L., Fu, C. X., Li, R., Qi, F. Y., Liu, Z. L., et al. (2024). Unveiling the crucial role of soil microorganisms in carbon cycling: a review. *Sci. Total Environ.* 909:168627. doi: 10.1016/j.scitotenv.2023.168627

Xiao, H. B., Li, Z. W., Chang, X. F., Deng, L., Nie, X. D., Liu, C., et al. (2018). Microbial CO_2 assimilation is not limited by the decrease in autotrophic bacterial abundance and diversity in eroded watershed. *Biol. Fertil. Soils* 54, 595–605. doi: 10.1007/s00374-018-1284-7

Xing, W., Lu, X. M., Ying, J. Y., Lan, Z. C., Chen, D. M., and Bai, Y. F. (2022). Disentangling the effects of nitrogen availability and soil acidification on microbial taxa and soil carbon dynamics in natural grasslands. *Soil Biol. Biochem.* 164:108495. doi: 10.1016/j.soilbio.2021.108495

Yan, J. F., Wang, L., Hu, Y., Tsang, Y. F., Zhang, Y. N., Wu, J. H., et al. (2018). Plant litter composition selects different soil microbial structures and in turn drives different litter decomposition pattern and soil carbon sequestration capability. *Geoderma* 319, 194–203. doi: 10.1016/j.geoderma.2018.01.009

Yang, J. Y., Cen, C. H., Wang, W. Z., Wang, Z. J., Gao, X. Y., and Jian, M. P. (2024). Alterations in carbon and nitrogen cycling mediated by soil microbes due to the conversion of karst mountainous forests into urban parks. *Catena* 245:108339. doi: 10.1016/j.catena.2024.108339

Yang, Y., Sun, H., Zhang, P. P., Wu, F., Qiao, J. B., Li, T. C., et al. (2023). Review of managing soil organic C sequestration from vegetation restoration on the loess plateau. *Forests* 14:1964. doi: 10.3390/f14101964

Yao, Y. W., Dai, Q. H., Gao, R. X., Yi, X. S., Wang, Y., and Hu, Z. Y. (2023). Characteristics and factors influencing soil organic carbon composition by vegetation type in spoil heaps. *Front. Plant Sci.* 14:1240217. doi: 10.3389/fpls.2023.1240217

Yao, Y., Wang, L. L., Hemamali Peduruhewa, J., Van Zwieten, L., Gong, L. X., Tan, B. C., et al. (2023). The coupling between iron and carbon and iron reducing bacteria control carbon sequestration in paddy soils. *Catena* 223:106937. doi: 10.1016/j.catena.2023.106937

Zhang, W. J., Munkholm, L. J., Liu, X., An, T. T., Xu, Y. D., Ge, Z., et al. (2023). Soil aggregate microstructure and microbial community structure mediate soil organic carbon accumulation: evidence from one-year field experiment. *Geoderma* 430:116324. doi: 10.1016/j.geoderma.2023.116324

Zhao, K., Kong, W. D., Wang, F., Long, X. E., Guo, C. Y., Yue, L. Y., et al. (2018). Desert and steppe soils exhibit lower autotrophic microbial abundance but higher atmospheric CO_2 fixation capacity than meadow soils. *Soil Biol. Biochem.* 127, 230–238. doi: 10.1016/j.soilbio.2018.09.034

Zhao, C., Long, J., Liao, H. K., Zheng, C. L., Li, J., Liu, L. F., et al. (2019). Dynamics of soil microbial communities following vegetation succession in a karst mountain ecosystem, Southwest China. *Sci. Rep.* 9:2160. doi: 10.1038/s41598-018-36886-z

Zheng, Z. C., Liu, B. Y., Fang, X., Fa, K. Y., and Liu, Z. (2022). Dryland farm soil may fix atmospheric carbon through autotrophic microbial pathways. *Catena* 214:106299. doi: 10.1016/j.catena.2022.106299

Zheng, F. J., Wu, X. P., Zhang, M. N., Liu, X. T., Song, X. J., Lu, J. J., et al. (2022). Linking soil microbial community traits and organic carbon accumulation rate under long-term conservation tillage practices. *Soil Tillage Res.* 220:105360. doi: 10.1016/j.still.2022.105360

Zhou, X., Tahvanainen, T., Malard, L., Chen, L., Pérez-Pérez, J., and Berninger, F. (2024). Global analysis of soil bacterial genera and diversity in response to pH. *Soil Biol. Biochem.* 198:109552. doi: 10.1016/j.soilbio.2024.109552

Zhou, Z. F., Wei, W. L., Shi, X. J., Liu, Y. M., He, X. H., and Wang, M. X. (2019). Twenty-six years of chemical fertilization decreased soil RubisCO activity and changed the ecological characteristics of soil *cbbL*-carrying bacteria in an entisol. *Appl. Soil Ecol.* 141, 1–9. doi: 10.1016/j.apsoil.2019.05.005

Zhou, L., Zhao, T. L., Thu, N., Zhao, H. M., Zheng, Y., and Tang, L. (2024). The synergistic effects of different phosphorus sources: Ferralsols promoted soil phosphorus transformation and accumulation. *Agronomy* 14:2372. doi: 10.3390/agronomy14102372

Zhu, X. Y., Fang, X., Xiang, W. H., Chen, L., Ouyang, S., and Lei, P. F. (2023). Vegetation restoration drives dynamics of soil nitrogen content and availability in the subtropics. *Catena* 220:106720. doi: 10.1016/j.catena.2022.106720